# L4-to-L4 nerve root transfer for hindlimb hemiplegia after hypertensive intracerebral hemorrhage

## From the Contents

Teng-Da Qian[1, #], Xi-Feng Zheng[2, #], Jing Shi[3], Tao Ma[3], Wei-Yan You[4], Jia-Huan Wu[4], Bao-Sheng Huang[5], Yi Tao[6], Xi Wang[7], Ze-Wu Song[7], Li-Xin Li[7, *]

**Graphical Abstract** *L4-to-L4 root transfer restores lower limb function after hypertensive intracerebral hemorrhage*
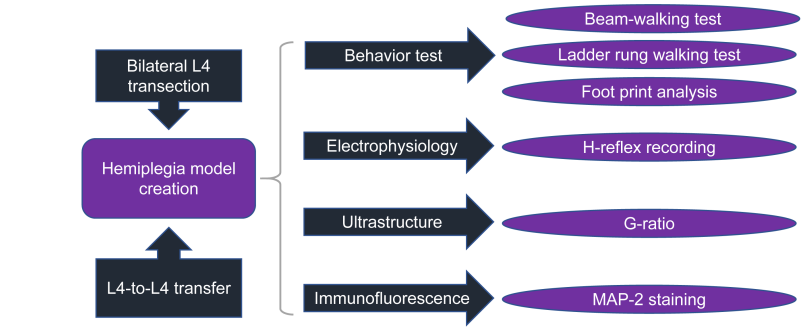


## Abstract

There is no effective treatment for hemiplegia after hypertensive intracerebral hemorrhage. Considering that the branches of L4 nerve roots in the lumbar plexus root control the movement of the lower extremity anterior and posterior muscles, we investigated a potential method of nerve repair using the L4 nerve roots. Rat models of hindlimb hemiplegia after a hypertensive intracerebral hemorrhage were established by injecting autogenous blood into the posterior limb of internal capsule. The L4 nerve root on the healthy side of model rats was transferred and then anastomosed with the L4 nerve root on the affected side to drive the extensor and flexor muscles of the hindlimbs. We investigated whether this method can restore the flexible movement of the hindlimbs of paralyzed rats after hypertensive intracerebral hemorrhage. In a beam-walking test and ladder rung walking task, model rats exhibited an initial high number of slips, but improved in accuracy on the paretic side over time. At 17 weeks after surgery, rats gained approximately 58.2% accuracy from baseline performance and performed ankle motions on the paretic side. At 9 weeks after surgery, a retrograde tracing test showed a large number of fluoro-gold-labeled motoneurons in the left anterior horn of the spinal cord that supports the L4-to-L4 nerve roots. In addition, histological and ultramicrostructural findings showed axon regeneration of motoneurons in the anterior horn of the spinal cord. Electromyography and paw print analysis showed that denervated hindlimb muscles regained reliable innervation and walking coordination improved. These findings suggest that the L4-to-L4 nerve root transfer method for the treatment of hindlimb hemiplegia after hypertensive intracerebral hemorrhage can improve the locomotion of hindlimb major joints, particularly of the distal ankle. Findings from study support that the L4-to-L4 nerve root transfer method can effectively repair the hindlimb hemiplegia after hypertensive intracerebral hemorrhage. All animal experiments were approved by the Animal Ethics Committee of the First Affiliated Hospital of Nanjing Medical University (No. IACUC-1906009) in June 2019.

**Key Words:** central hemiplegia; end-to-end anastomosis; functional regeneration; hypertensive intracerebral hemorrhage; L4 nerve root; neural regeneration; neurotization; rat model; reinnervation; skilled restoration

Chinese Library Classification No. R493; R361; R364

## Introduction

Hypertensive intracerebral hemorrhage (HICH) can cause catastrophic, life-changing damage; it has an annual incidence of approximately 150 in 100,000 worldwide, and > 81.3% of cases include severe hemiplegia in the contralateral limbs (Ahamed and Sreejit, 2019; Ettenhofer et al., 2019; Fernando et al., 2019; Zhu et al., 2020). Patients with limb motor dysfunction significantly lose their self-help ability, which impedes social engagement and places burden on the family (Rivera-Lara et al., 2018; Chen and Chang, 2020; Perin et al.,

[1]Department of Neurosurgery, Jintan Hospital, Affiliated Hospital of Jiangsu Vocational College of Medicine, Jintan, Jiangsu Province, China; [2]Department of Gastroenterology, Jintan Hospital, Affiliated Hospital of Jiangsu Vocational College of Medicine, Jintan, Jiangsu Province, China; [3]Department of Neurosurgery, Changzhou First People's Hospital, Suzhou University, Changzhou, Jiangsu Province, China; [4]Deparment of Neurobiology, Basic Medical College, Nanjing Medical University, Nanjing, Jiangsu Province, China; [5]Department of Neurosurgery, Sir Run Run Hospital Affiliated to Nanjing Medical University, Nanjing, Jiangsu Province, China; [6]Department of Neurosurgery, Affiliated Cancer Hospital of Nanjing Medical University, Nanjing, Jiangsu Province, China; [7]Department of Neurosurgery, First Affiliated Hospital of Nanjing Medical University, Nanjing, Jiangsu Province, China

*Correspondence to: Li-Xin Li, PhD, lilixin2@hotmail.com.
https://orcid.org/0000-0002-9404-5538 (Li-Xin Li)
#Both authors contributed equally to this work.

2020; Schiavo et al., 2020; Niama Natta et al., 2021; Simpson et al., 2021). Conventional interventions for hemiplegia after HICH include physical rehabilitation or physiotherapy (Chiaramonte et al., 2020; Hirano and Nitta, 2020; Park et al., 2020; Wang et al., 2020). Nevertheless, outcomes are usually dissatisfactory, which has spurred the search for effective patient-oriented therapies.

Many studies conducted in both humans and rodents have demonstrated that an injured brain cortex can regain control of the contralateral limbs through neural network remodeling across the perilesional regions and contralesional hemisphere after rewiring an afferent circuit (Zheng et al., 2018a, b; Kikuta et al., 2020; Tuffaha et al., 2020). Recently, peripheral nerve transfer, which can stimulate compensatory cerebral plasticity, has been reported to rescue partial knee extension or hand prehension in patients with acute flaccid myelitis or central nervous system diseases (Yorukoglu and Gurkan, 2018; Doi et al., 2019; Lee et al., 2019; Nath and Somasundaram, 2019). Although neurotization is still in the early stage for treatment use and needs to be refined (Pino et al., 2019; Yu et al., 2020), its demonstrated success has inspired us to investigate its efficacy for hindlimb paralysis after HICH, and its potential as a therapeutic candidate to promote functional recovery.

Currently, there are few data on neurotization for hindlimb hemiplegia after HICH; only several types of nerve transfer, such as L6-to-L6, L4-to-L5, and L3-to-L4 in animals, as well as obturator nerve to femoral nerve in humans, have been reported to repair paralyzed hindlimbs after central nervous system disease onset (Lin et al., 2013; Zong et al., 2016; Tiwari et al., 2019; Bao et al., 2020). Disappointingly, only weak and rough motions were observed in the proximal major joints (i.e., hip and knee), with no activity observed in the distal joints (i.e., ankle). These poor outcomes likely result from an inadequate option for a source nerve. Anatomically, fine motor activity requires coordination between flexors and extensors chiefly composed of antero-posterior muscle groups (such as, quadriceps femoris, semimembranosus, gastrocnemius, and tibialis anterior) in the lower extremity. The L4 root innervates these muscles, which drive distal joint activity. In brief, the L4 nerve root bifurcates to form both the femoral and sciatic nerves and is theoretically considered as an optimal donor nerve. At the spinal cord level, all lumbar plexus nerve roots are connected through a neural network composed of intermediate neurons. When one nerve root is injured or severed, the other intact nerve roots can provide effective functional compensation to ensure normal operation of the target organ. However, even if the intrinsic role of the L4 nerve root before transection can be undertaken by other lumbar roots after transection, experimental analyses in rodents and humans are needed to determine the potential of the L4 nerve root as a therapeutic candidate.

Thus, in the present study, we established the L4-to-L4 transfer prototype in a rat model, in which we investigated the effects of the neurotization on recovery of the paralyzed hindlimb after HICH.

## Materials and Methods

### Ethics statement
We conducted all animal experiments in accordance with the principles and procedures outlined in the NIH Guide for the Care and Use of Laboratory Animals (National Academies Press, 2011), enforced animal procedures approved by the Institutional Animal Care and Use Committee at Nanjing Medical University (Nanjing, Jiangsu Province, China; approval No. IACUC-1906009) in June 2019, and performed all surgical procedures after rats were anesthetized with 2% pentobarbital sodium (40 mg/kg; Nanjing Senbeijia Biological Technology Co., Ltd., Nanjing, Jiangsu Province, China). All attempts were made to minimize animal suffering.

### Animals
Thirty Sprague-Dawley male rats, weighing 250–300 g, purchased from the Laboratory Animal Center at Nanjing Medical University (license No. SYXK (Su)-2018-0020), were included in this study. They were housed three per cage in a controlled animal facility that was kept at a constant temperature of 22 ± 1°C and a relative humidity of 60 ± 10% with water and food *ad libitum*. The animal care unit was sustained at a 12-hour light/dark cycle with lights on at 7:00 a.m. All rats were randomly assigned into three groups with 10 rats each. The sham-operation group was subjected to sham operation. The Bi-L4 transection group received bilateral L4 transection. The L4-L4 transfer group underwent L4-to-L4 root transfer following a hematoma-driven lesion in the posterior limb of the internal capsule (PLIC). All rats were kept in a noiseless room.

### Establishment of an internal capsule insult
Using published nerve tracings as a guide (Frost et al., 2013; Song et al., 2017), we created a hematoma-caused lesion in the posteromedial area of the PLIC. Rats were anesthetized with 2% pentobarbital sodium intraperitoneally with body temperature maintained at 37 ± 0.5°C using a heating pad. Briefly, after rats were restrained in a stereotactic frame (RWD-68025, Shengzheng Biotechnology Co., Ltd., Nanjing, Jiangsu Province, China), a scalp incision was made along the midline, hemostasis was performed using a bipolar electrocoagulator (Johnson & Johnson Medical Devices Co., Ltd., Suzhou, Jiangsu Province, China), and then a small hole was drilled on the skull. Subsequently, a hydraulic microinjector was gradually inserted perpendicularly into the target area (anteroposterior, –3.1 from bregma; mediolateral, ±3.3 from the midline; dorsoventral, –7.8; $n$ = 30) (**Figure 1A** and **B**). Approximately 180 μL blood or saline was slowly injected into the target site for 15 minutes at a rate of 12 μL/min through a 30G Hamilton syringe connected to an UltraMicroPump (WPI, Sarasota, FL, USA). The sham-operation group received a saline injection, followed by exposure of only bilateral L4 nerve roots. After surgery, all rats were transported to a recovery chamber with ketoprofen (2 mg/kg, i.m.) for analgesia for 3 consecutive days. Seven days after injection, T2-weighted magnetic resonance imaging (MRI) was used to locate the affected area (**Figure 1C**). Both behavioral and electromyographic tests confirmed the establishment of the rat model.

### Selection of a donor nerve
In a preliminary experiment, 24 naïve rats, weighing 250–300 g, were classified into two groups ($n$ = 12 rats/group). In one group, unilateral L4 root was excised sharply, without transection of other lumbar roots, whereas in another group, the L4 root was retained and the other lumbar roots (L2, L3, L5, and L6) were excised completely. After surgery, all rats received an intramuscular injection of penicillin (80,000 U per day) for 3 days, underwent application of lidocaine ointment to the incision for 5 days, and underwent observations and measurements in a blinded fashion. Seven days later, behavioral and electromyographic tests were performed to confirm eligibility of the L4 nerve root as a donor target.

### Behavioral tests
A beam-walking test, ladder rung walking task, and footprint analysis were performed as per the established protocols at baseline, 9, 13, and 17 weeks post-operation (Kemp et al., 2010). At 15 days before the baseline valuations, rats were trained on each procedure. A schematic illustration of the corresponding protocol is shown in **Figure 1D**.

For the beam-walking test, rats ($n$ = 10/group) were trained before the surgery to cross a horizontal beam. A single run

was deemed as satisfactory if the animal walked across the beam continuously at a constant gait. Nine satisfactory runs for each animal were used to calculate their performance in a blinded manner by an experienced reviewer. The number of times that an animal slipped off the ledge with its affected hindlimb was recorded and then normalized to the sum of steps taken. Slips onto the ledge were rated as a full slip (given a score of 1) and a half slip (given a score of 0.5) was scored if the hindlimb touched one side of the beam. The slipping rate was designated as the number of slips per the sum of right hindlimb steps.

For the ladder rung walking task, rats ($n$ = 10/group) were trained before surgery to travel across a horizontally-placed ladder from a neutral cage to their home cage. Traveling across the ladder at a uniform velocity was considered a satisfactory run, and nine satisfactory runs per animal were collected for their performance calculations. The slipping rate was evaluated as the number of slips per the sum of right hindlimb steps.

For the footprint analysis, rats were trained to walk straight across a gangway three times for acclimatization. Subsequently, rats were tested on a gangway covered with white paper, with a black cage at the end. The right forepaw and hindpaw were coated with blue and red ink, respectively. Unclear and partial paw prints were excluded from the analysis. The rats were placed individually in an open field (90 cm × 150 cm) and observed for 5 minutes to rate hindlimb activity from 0 to 21 using the Basso, Beattie and Bresnahan (BBB) rating scale.

### L4 nerve root surgery procedures

At 2 weeks after establishment of the rat hemiplegia models, L4-to-L4 nerve root transfer was performed in the L4-L4 transfer group, bilateral L4 nerve root transfection was conducted in the Bi-L4 transection group, and exposure of bilateral L4 nerve root only was performed in the sham-operation group. After ether inhalation and anesthesia by an intraperitoneal injection of 2% pentobarbital sodium, rats were laid in supine position, shaved, and fixed on the miniature operation table. A median incision (3–4 cm long) was made longitudinally in the abdomen, which was centered on the L4 and paralleled the anterior superior iliac spine. Bilateral L4 nerve roots were observed under the operating microscope (SZ61, Olympus, Tokyo, Japan). For the L4-to-L4 root transfer, the left L4 root (intact side) was traced and transected as distally to the intervertebral foramen as possible, whereas the right L4 root was severed as proximally as possible. The proximal stump of the left L4 nerve root was transferred to the distal stump of the right L4 root using 10-0 Prolene sutures, with the right proximal stump secured to the ambient psoas major. In the bi-L4 transection group, the stumps of bilateral L4 nerve roots were fixed to the muscle to avoid neural reconnection (**Figure 1E** and **F**). An absorbable hemostatic sponge was carefully stuffed around the operative field before strict skin closure.

### T2-weighted MRI for localization

At 7 days after blood injection, T2-weighted MRI showed the PLIC lesion on a Bruker Biospec 7-T MRI system (Bruker, Karlsruhe, Germany). Rats were anesthetized with 5% halothane and maintained with 2% halothane (in 30% O$_2$: 70% N$_2$O, v/v), and were then intubated and mechanically ventilated at 65 beats/min. A T2-weighted image of the lesion obtained at 1 second was acquired.

### Electrophysiological evaluation
#### Electromyographic examination

At 5 days after the left PLIC insult, surface electromyogram was conducted to verify the rat model. After mild anesthesia with 2% pentobarbital sodium, rat bilateral lower limbs were

shaved. A reference electrode and a recording electrode were placed on the lateral and medial thigh of the hindlimb, respectively. Rats were stimulated at an increasing intensity of current from 0.5 mA to 1 mA, with self-adhesive electrodes in place. Because of the neuroanatomic association in lower extremities, we performed serial electromyography with a concentric needle in the anterior-posterior muscle groups 10 days after severing the lumbar root. Myokymic potentials and positive sharp waves were recorded to locate the muscles from the L4 nerve root. The data were collected under the conditions of excision of only the L4 nerve root or retention of only the L4 nerve root.

At 9, 13, and 17 weeks after transfer, acupuncture electromyogram was performed to assess the L4-supplied muscles for early neurogenic or compound muscular action potential (MUAP) changes, in addition to the denervated potentials. Additionally, positive sharp waves without myokymic potentials as a confounding variable were excluded, neurogenic or myogenic alterations of MUAPs were assessed, and a reinnervated potential in the investigated muscles was detected at a scheduled time.
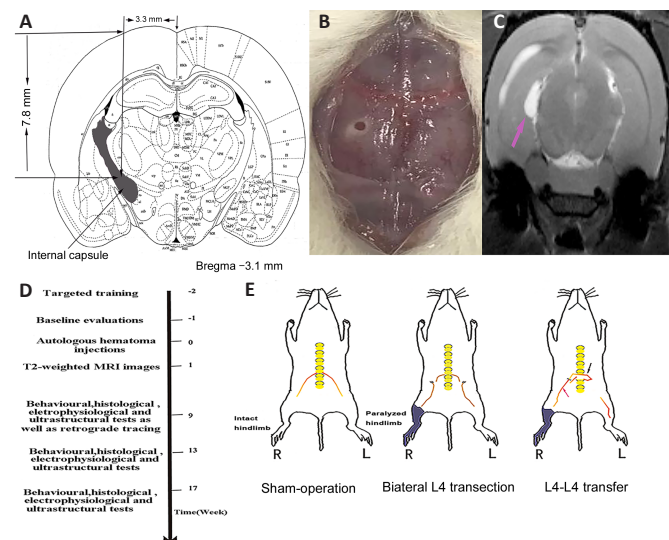


**Figure 1 | Diagram of establishment of rat models and treatments for each group.**
(A) The coordinates were determined according to an illustration by Paxinos and Watson (Paxinos et al., 1980). (B) A hole 0.8 mm in diameter was created in the rat cranium, 3.1 mm posterior to the bregma and 3.3 mm lateral to the midline. (C) A coronal T2-weighted magnetic resonance imaging (MRI) image indicates the hematoma in the posterior limb of the left internal capsule (pink arrow). (D) The experimental outline. (E) Sham-operation was conducted in the sham-operation group (bilateral L4 nerve roots were not severed intraoperatively, $n$ = 10). (F) Bilateral L4 nerve roots were sharply transected in the Bi-L4 transection group ($n$ = 10), and the stumps were secured to the psoas major muscles or capped with soft tissues. (G) The L4-to-L4 transfer was performed in the L4-to-L4 root transfer group ($n$ = 10). Contralesional L4 was resected as distally as possible, and the ipsilesional L4 was severed proximally. Interrupted suture was applied to anastomosis of stumps. L: Left; R: right.

### H-reflex recording in the gastrocnemius

After the aforementioned preparations, a pair of receiving electrodes was introduced into the gastrocnemius in the right hindlimb and a stimulating electrode was placed transcutaneously behind the medial malleolus. All of the electrodes were linked with a four-channel electrophysiology instrument (Galileo NT LineKey, Florence, Italy). The reinnervated nerve was stimulated using a single pulse (2 ms, 5 Hz) at an initial current of 0.1 mA, with 0.1 mA increments until reaching the maximum current. The latencies for H-wave and M-wave were determined.

### Immunofluorescence for regenerated nerves

Rats were intraperitoneally injected with an overdose of 2% pentobarbital sodium and were transcardially perfused with 600 mL of saline and 400 mL of 4% paraformaldehyde solution. The regrowing section of the regenerating nerve, 5 mm away from the coaptation site, was resected rostrally and caudally, immersed into 4% paraformaldehyde overnight at 4°C, followed by 30% sucrose in 0.1 M phosphate buffer overnight at 4°C, and then sliced longitudinally at a thickness of 20 μm with a manual rotary microtome (LEICA CM1905; Leica, Wetzlar, Germany). Every fourth section (three sections per segment) was chosen for immunofluorescence. Next, the specimens were incubated with microtubule-associated protein-2 (MAP-2; Abcam, Cambridge, MA, USA) diluted at 1:250 in primary antibody dilution buffer and then placed on a reciprocal shaker running overnight at 4°C. The primary antibody was skipped in the negative control. Following MAP-2 incubation, the tissue sections were carefully washed in 0.01 M phosphate buffered saline, incubated with Alexa Fluor-693 (1:250; Sigma, St. Louis, MO, USA) at 37°C for 30 minutes, treated with an anti-quenching reagent and then quickly photographed under a fluorescence microscope (LEICA DM2500). The regenerated connectivity at the anastomosis site can be calculated using immunofluorescence if the regrowing axons are labeled with MAP-2 at the point of interest. The connectivity rate was calculated as the transverse diameter for the regenerated nerve divided by that for the nerve root at the coaptation point.

### Retrograde tracing of the motoneurons to the quadriceps femoris

At 9, 13 and 17 weeks after transfer, the quadriceps femoris on the paretic side in parallel with severance of other lumbar roots (i.e., L2, L3, L5 and L6) was surgically exposed and 1 μL 4% fluoro-gold (UE-F4040) was injected at three locations. After saline washes, the incision was finally closed. In naïve rats, an equal amount of 4% fluoro-gold was injected into the quadriceps femoris in the intact hindlimb for a control. Seven days later, the lumbar spinal cord from the L4-to-L4 nerve root was sectioned at 20 μm thickness and photographed using confocal microscopy (Zeiss LSM880 with NLO & Airyscan, Manchester, UK). Soma and partial dendritic arbors labeled with fluoro-gold were photographed. Using a 10× objective lens and 50-μm photograph separation, the labeled motoneurons were captured at a 480-nm wavelength. Z-stack was used to reconstruct the optical sections.

### Ultrastructural assessment for the regrowing nerve

To examine the reinnervated dynamics, the regrowing roots, 3 mm from the coaptation site, were transected rostrally and caudally for ultrastructural evaluation at 9, 13 and 17 weeks. Briefly, the nerve sections were fixed in 2.5% glutaraldehyde, dehydrated in both graded ethanol and propanone, and permeated with resin. Next, the specimens were subjected to longitudinal and transverse ultrathin slices and stained with 3% uranyl acetate-lead citrate. Ultrastructure of the regenerated axons was captured at various resolutions using FEI (Tecnai Spirit Biotwin, Waltham, MA, USA). The g-ratio was calculated as the axon diameter divided by the fiber diameter as an index of the regenerated size. Multiple calculations were made per axon and the G-ratio was considered a reliable parameter reflecting axon remyelination.

### Statistical analysis

All data were analyzed with SPSS 21.0 software (IBM, Armonk, NY, USA) and ImageJ software (1.52p, National Institutes of Health, Bethesda, MD, USA) and expressed as the mean ± SEM. Differences between groups were calculated using repeated-measures analysis of variance and one-way analysis of variance followed by least significant difference *post hoc* test. The statistical significance value was set at a *P* value of 0.05 or lower.

## Results

### Identification of a right hindlimb paralysis

At 7 days after injury to the dorsomedial area of PLIC, rats began to exhibit reduced activity in the right lower extremity and galloped in circles centered on the right hindlimb. In the walking tasks, there was a > 85% slip rate in the right hindlimb compared with the left hindlimb (**Figure 2A** and **B**). In the footprint analysis, the forepaw and hindpaw prints on the paretic side were non-overlapping for at least 6 months, with a spacing of 19.2 ± 0.7 mm (**Figure 2D**). In contrast, the spacing on the intact side had a very small interval 1.2 ± 0.1 mm (**Figure 2C**).

Additionally, denervated MUAPs in the hemiplegic hindlimb had a lengthened duration and shortened amplitude (**Figure 2F**) compared with those in the left hindlimb (**Figure 2E**), which is consistent with the results of the footprint analysis. The results imply a successful establishment of a rat model of hemiplegia after HICH.

### Eligibility of L4 nerve root as a donor nerve

Anatomically, a nerve root that controls flexors and extensors is usually considered as an optimal donor candidate. We performed initial experiments to screen a donor nerve. At 10 days after transection of L4 only, acupuncture electromyography showed that myokymic potentials and positive sharp waves were prominently detected in the quadriceps femoris, moderately detected in the semimembranosus and gastrocnemius, slightly detected in the tibialis anterior, and hardly detected in the biceps femoris (**Figure 3A**). In contrast, in the condition of retention of the L4 nerve root and excision of other lumbar roots, normal potentials were observed in the corresponding muscles, particularly in the quadriceps femoris, semimembranosus, gastrocnemius, and tibialis anterior (**Figure 3B**). The maximum BBB scores were 20 and 13 for transection of the right L4 nerve root only and retention of the right L4 only, respectively (**Figure 3C**). The BBB scores suggested that under the condition of retention of the L4 nerve root only, the hindlimb function might recover to approximately 70% of a naïve state within 2 weeks. Electromyography indicated that the muscles controlled by L4 could perform flexion and extension for major joints in the hindlimb, especially for the ankle. These results demonstrated eligibility of the L4 nerve root as a source nerve.

### Behavioral assessment

The right forepaw and hindpaw prints from the footprint analysis of a naïve rat and model rat are shown in **Figure 4A**, and the intervals between the forepaw and hindpaw prints on the affected side are shown in **Table 1**. In the L4-L4 transfer group, the interval between the forepaw and hindpaw prints during L4-to-L4 root transfer significantly diminished over time until an overlapping status emerged at 17 weeks after surgery (**Figure 4B**). In the beam-walking test and ladder rung walking task, the overall slip rate for the bilateral hindlimbs did not statistically differ between the bilateral (Bi)-L4 transection and L4-L4 transfer groups and attained 90% at baseline (**Figure 4C** and **D**).

**Table 1 | Interval between forepaw and hindpaw prints on the affected side (mm)**

| Group | 9 wk after transfer | 13 wk after transfer | 17 wk after transfer |
|---|---|---|---|
| Sham-operation | 19.5±0.7 | 19.2±0.9 | 18.9±0.5 |
| Bi-L4 transection | 22.3±0.4 | 20.8±0.5 | 19.6±0.3 |
| L4-L4 transfer | 20.3±0.8# | 14.7±0.9# | 5.6±0.2 |

Data are expressed as the mean ± SEM (*n* = 10; repeated-measures analysis of variance). #*P* < 0.05, *vs.* 17 wk after transfer. Bi: Bilateral.

At 1 week, the slip rate in the Bi-L4 transection group drastically declined to 44–56% as compared with that of the L4-L4 transfer group. At 3 weeks, rats in the sham-operation group achieved approximately 95% accuracy, in contrast to approximately 57% accuracy in the Bi-L4 transection group and approximately 13% accuracy in the L4-L4 transfer group. At 5 weeks, in the Bi-L4 transection and L4-L4 transfer groups, behavioral improvement was observed, with greater improvement observed in the Bi-L4 transection group. From 9 weeks onward, rats in the L4-L4 transfer group displayed greater reductions in the slip rate than did those in the Bi-L4 transection group. Although an increase in accuracy was observed after 9 weeks, rats in the Bi-L4 transection and L4-L4 transfer groups did not improve to the level of the sham-operation group at any time point. The BBB score in the L4-L4 transfer group was significantly higher at 17 weeks than at 9 and 13 weeks (**Figure 4E**). The data suggest effective motor function recovery of the hemiplegic hindlimb after L4-to-L4 root transfer.

**Electrophysiological evaluation of contralateral L4 transfer**
In the L4-to-L4 root transfer group, the reinnervated MUAPs could be elicited with concentric needles in the quadriceps femoris, semimembranosus, lateral gastrocnemius and tibialis anterior of the right hindlimb in 4 out of 10 rats (40%) at 9 weeks, in 7 rats (70%) at 13 weeks, and in 9 rats (90%) at 17 weeks after surgery (**Figure 5A** and **B**). Also, the denervated MUAPs detected in the target muscles markedly decreased over time. In H-reflex recordings, the M/H-wave latency for the right gastrocnemius was remarkably longer at 9 weeks than that at 17 weeks ($P < 0.05$) (**Table 2** and **Figure 5C**). The latency shortened over time until it reached an approximately normal level ($P > 0.05$). Together, the results suggested that the L4-to-L4 nerve root transfer efficiently reinnervated the targeted end-organs (**Figure 5**).
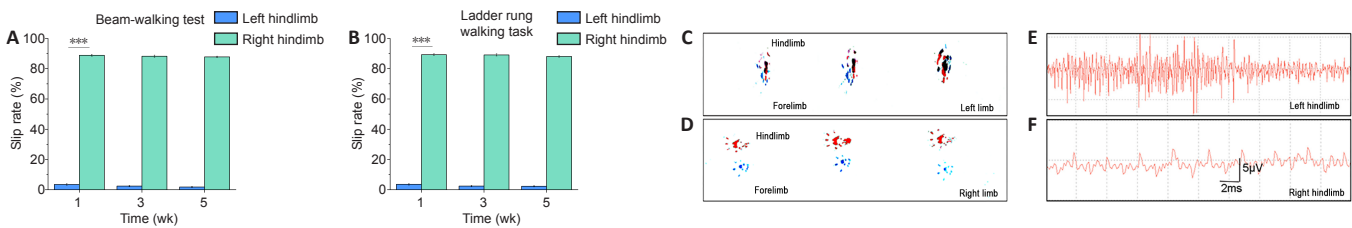


**Figure 2 | Behavioral and electromyographic assessments confirming establishment of the rat model.**
(A and B) In the beam-walking test and ladder rung walking task, a > 85% slip rate was observed in the right hindlimb (affected side), compared with that in the left hindlimb (intact side). Data were expressed as the mean ± SEM ($n = 10$; repeated-measures analysis of variance). ***$P < 0.001$. (C) Superposed forepaw and hindpaw prints, characteristic of a naïve rat, were presented as a reference. (D) A contralateral detached state was present in rats with an injury to the posteromedial area of posterior limb of the internal capsule. In this case, normal muscular action potentials (E) were replaced with the denervated ones (F).
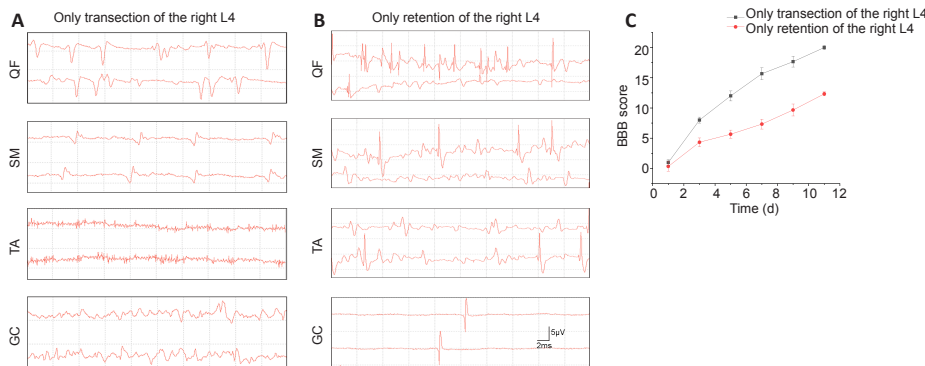


**Figure 3 | Availability of L4 as a source nerve.**
(A) Positive waves or denervated potentials occurred in the QF, SM, TA, and GC. (B) Normal muscular action potentials were recorded from the same target muscles. (C) BBB scores differed between the two treatments. Data are expressed as the mean ± SEM ($n = 10$; repeated-measures analysis of variance). BBB: Basso, Beattie and Bresnahan rating scale; GC: gastrocnemius; QF: quadriceps femoris; SM: semimembranosus; TA: tibialis anterior.
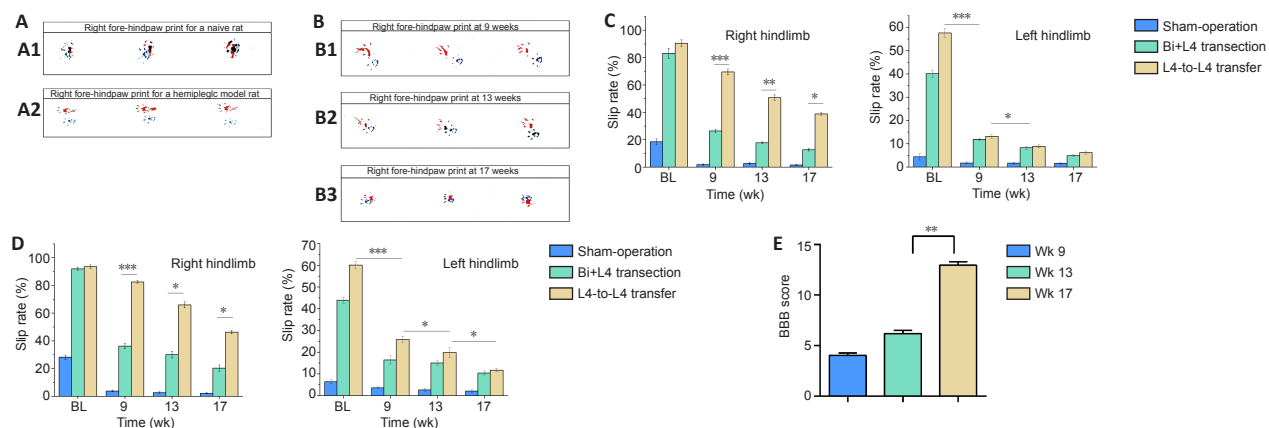


**Figure 4 | Behavioral improvements following the L4-to-L4 transfer.**
(A) Representative forepaw and hindpaw prints for a naïve rat (A1) and model rat (A2). (B) Data at 9 weeks (B1), 13 weeks (B2), and 17 weeks (B3) after L4-to-L4 nerve root transfer indicate that the nonoverlapping status was gradually pulled into an overlap post-procedure. (C, D) In the beam-walking test (C) and ladder rung walking task (D), there was no significant difference in accuracy at baseline between the bilateral (Bi)-L4 transection and L4-L4 transfer groups. With time, a larger decline in slip rate on the affected side was observed in the L4-L4 transfer group than in the Bi-L4 transection group. In the L4-L4 transfer group, there was also a relatively higher slip rate on the intact side compared with that in the sham-operation group, owing to body imbalance. Improvement in accuracy was observed at later time points. (E) Eventually, at 17 weeks after transfer, rats in the L4-L4 transfer group scored approximately 13 on the BBB scale. These results suggest a positive effect of the intervention on motor function. Data were expressed as the mean ± SEM ($n = 10$; C, D: repeated-measures analysis of variance; E: one-way analysis of variance followed by the least significant difference *post hoc* test). *$P < 0.05$, **$P < 0.01$, ***$P < 0.001$.
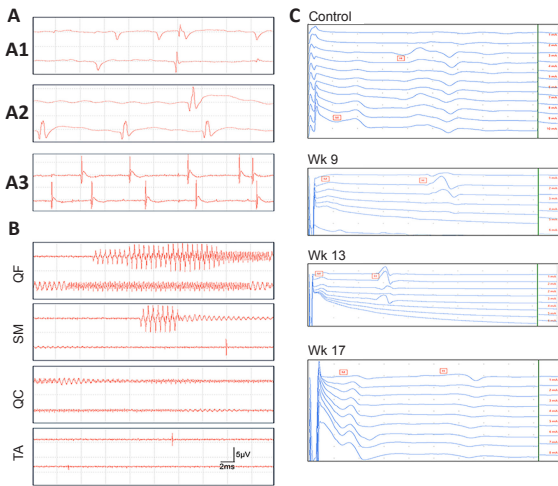
**Figure 5 | Electromyographic assessment demonstrating reinnervation of the denervated muscles.**
(A1) At 9 weeks after transfer, many positive sharp waves were observed ($P > 0.05$). (A2) Muscular action potentials began to appear and positive sharp waves disappeared. (A3) Numerous muscular action potentials were detected ($P > 0.05$). (B) The reinnervated potentials were prominently detected in the QF, moderately detected in the SM and QC, and slightly detected in the TA ($P > 0.05$). (C) H-reflex was evoked in a naïve rat as a control. At 9, 13, and 17 weeks after transfer, the H-reflex was markedly elicited in the gastrocnemius of the affected hindlimb, the latency of which shortened over time and reached an approximately normal latency. GC: gastrocnemius; QF: quadriceps femoris; SM: semimembranosus; TA: tibialis anterior.

**Table 2 | Latencies (ms) for M-wave and H-wave in the right gastrocnemius at different groups**

| Parameters | Control | 9 wk after transfer | 13 wk after transfer | 17 wk after transfer |
|---|---|---|---|---|
| M-wave | 2.09±0.19 | 3.26±0.21 | 2.78±0.16 | 2.11±0.19# |
| H-wave | 7.49±0.24 | 13.79±0.37 | 13.45±0.35 | 10.78±0.26# |

Data are expressed as the mean ± SEM ($n = 10$; repeated-measures analysis of variance). #$P < 0.05$, vs. 17 wk after transfer.

## Fluorogold-labeled motoneurons in the ventral horn from the L4-to-L4 root

In the ventral horn, many fluorogold-labeled motoneurons were observed (**Figure 6A**). At 9, 13, and 17 weeks (**Figure 6B–E**), the number of labeled motoneurons increased over time, in contrast to the contralateral side at the same time points ($P < 0.05$ for each time point). These results showed that an increasing number of regenerated axons reinnervated the motor endplates.
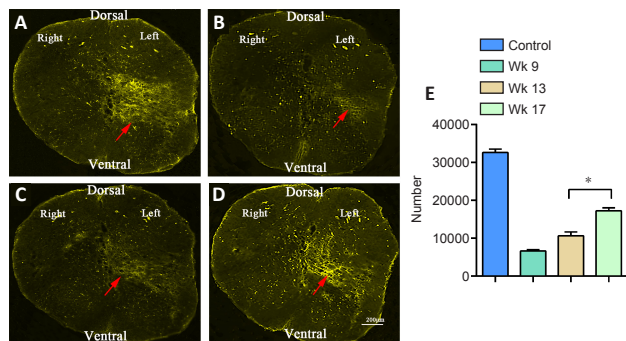


**Figure 6 | Retrograde tracing showed fluoro-gold-labeled motoneuron number increased over time.**
To assess the ability of the L4-to-L4 nerve root to transmit signals, a control group (A) was designed for quantitative comparison. At 9 weeks (B), 13 weeks (C), and 17 weeks (D) after transfer, many labeled motoneurons were observed in the ventral horn, and the labeled area increased over time. (E) Quantification of fluoro-gold-labeled motoneurons. Data were expressed as the mean ± SEM ($n = 10$; one-way analysis of variance followed by the least significant difference post hoc test). *$P < 0.05$.

## Immunofluorescence staining and ultrastructure of the reinnervated nerve root

At the coaptation site, regrowing axons were observed, with MAP-2-labeled axons accounting for 25.61 ± 5.18% at 9 weeks, 38.52 ± 3.64% at 13 weeks, and 57.89 ± 6.25% at 17 weeks (**Figure 7**) of all axons. Additionally, reinnervation between the stumps increased at each time point until reaching nearly complete reinnervation at 17 weeks ($P > 0.05$). Myelinated and unmyelinated axons were observed with ultrastructural analysis, further indicating progressing axon regeneration over the three time points ($P < 0.05$) (**Figure 8**). Over time, the G-ratio for regrowing axons declined, in parallel with an elevation of myelinogenesis. Additionally, more reinnervated axons were observed in a realigned and rearranged manner. The results demonstrated effective regeneration of nerve fibers.
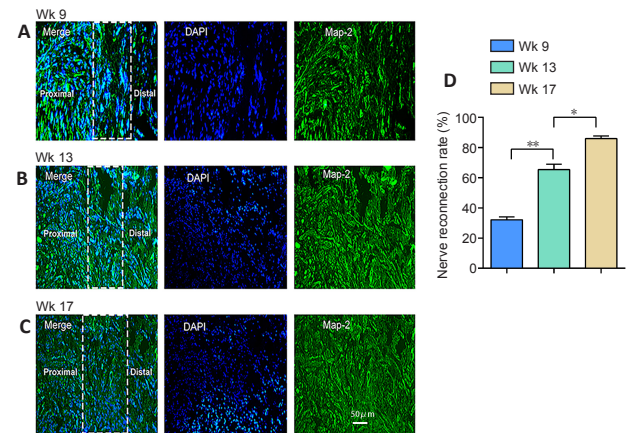


**Figure 7 | Immunofluorescence showed axon regeneration.**
Varying levels of immunostaining were observed in the reinnervated nerve roots collected at three time points after MAP-2 labeling. Dotted boxes indicate axon regeneration at the anastomosis site. Only partial regenerative reconnection occurred at the early stage after surgery (A and B). However, almost complete reconnection was observed at 17 weeks (C) after transfer. (D) The regenerated connectivity at the coaptation site. Data are expressed as the mean ± SEM ($n = 10$; one-way analysis of variance followed by the least significant difference post hoc test). *$P < 0.05$, **$P < 0.01$. MAP-2: Microtubule associated protein-2.
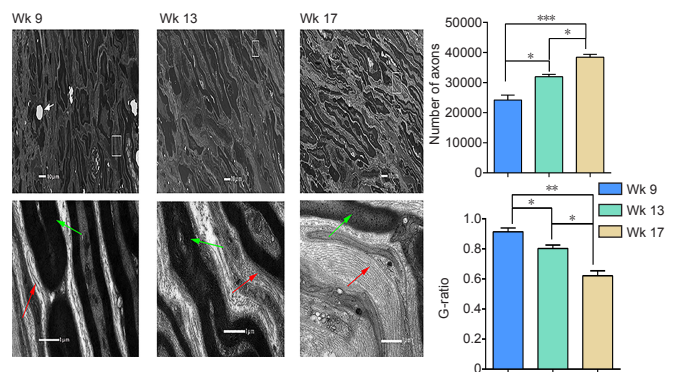


**Figure 8 | Ultrastructure demonstrating axon regrowth and remyelination.**
Varying levels of regeneration and myelinogenesis were observed at three time points. At 9 weeks, obvious axon necrosis or myelin sheath cell apoptosis was observed (white arrow). Marked remyelination (green arrow), vast axon regrowth (red arrow), and alignment of regenerated axons were observed at 17 weeks, in comparison with those at 9 and 13 weeks after transfer. Data are expressed as the mean ± SEM ($n = 10$; one-way analysis of variance followed by the least significant difference post hoc test). *$P < 0.05$, **$P < 0.01$, ***$P < 0.001$. The G-ratio declined over time.

## Discussion

Given the large number of people affected by HICH and the unsatisfactory outcomes, new interventions are needed for limb hemiplegia (Herweh et al., 2017; Chamudot et al., 2018; Fan et al., 2020; Jovanovic et al., 2020). The rationales

behind the C7-to-C7 transfer for the paretic upper limb are beginning to be accepted and understood as scalable (Fox et al., 2019; Yu et al., 2019a, b; Li et al., 2020; Yang et al., 2020). Reinnervation of the denervated muscles, γ-circuit interruption, and establishing a new pathway remarkably contribute to motor recovery after transfer (Sananpanich et al., 2018; Afshari et al., 2019). Contralateral lumbar neurotization engaging similar mechanisms was considered as an option for lower limb paresis after central neurological injury. Thus, in this study, we investigated the effect of L4-to-L4 transfer for hindlimb hemiplegia in rats.

There are several reasons why the L4 nerve root was identified as an optimal source nerve. First, transecting the L4 nerve root may not impair lower extremity motion, as shown by the BBB score, because of compensation from neighboring roots. Second, biomechanically, coordination between flexors and extensors leads to stable and refined movement. Anatomically, L4 simultaneously drives anteroposterior muscle groups, initiating robust flexion and extension in the hindlimb. Third, given the muscles innervated by L4, including the quadriceps femoris, semimembranosus, gastrocnemius, and tibialis anterior, it was inferred that L4 may not only control proximal joint activity but also distal joint motion in the lower limb. Thus, L4 as a donor nerve may have the best potential as a therapeutic candidate for functional recovery following nerve transfer, in comparison with other lumbar nerves.

In our study, we severed the efferent pathway via damage to the posteromedial area of PLIC to establish a successful rat model, as indicated by electromyography and paw print tests. Only slight or no spasm was observed in the model rat. We also investigated the potential of the L4-to-L4 transfer for motor recovery. A denervated muscle may atrophy if a nerve fiber fails to reinnervate within a certain time, i.e., 3 to 6 months. The results from H-reflex and retrograde tracing indicate that the regenerated axons had strongly reinnervated the target muscles. Additionally, the shortened latency for the M/H-wave and g-ratio over time led us to strongly speculate that nearly all regrowing fibers were myelinated and functional. Finally, we observed increasing regeneration between stumps, which we believe suggests that an increasing number of regenerated fibers reached the motor end-organ to generate better functional outcomes. Together, these findings suggest that after surgery, the axons regenerated and reinnervated the target muscles before muscle atrophy occurred.

We also observed distinct differences between the L4-to-L4 transfer and other previously published transfer modalities. After contralateral L4 transfer, rats could conduct large-range, dexterous, and strong activity in the distal major joints, such as the hip and knee joints. Additionally, in the ankle joint, full flexion and extension were often seen at the early stage, as indicated by the beam-walking test and ladder rung walking task. In contrast, in previous studies of other types of lumbar nerve transfer (such as L5-to-L6, L6-to-L6 and L4-to-L5), only rough motion in the proximal joints was observed, and skilled activities were barely observed for the major joints in the paretic hindlimb (Bao et al., 2020; Yang et al., 2021). A possible explanation for the different outcomes is that the L4 root controls the anteroposterior muscle groups, and is responsible for flexion and extension for the major joints in the hindlimb, whereas other lumbar nerves are not.

Central neurological injuries commonly cause motor control deficits in the whole leg, particularly in fine motor control. To achieve skilled locomotion, rats balance their weight and place limbs rapidly. Hence, fine muscle control, leg coordination, and the ability to achieve weight-bearing stepping movements are required for a successful performance in the beam-walking test and ladder rung walking task. Because of these coordinating factors, movement accuracy and gait were provisionally negatively impacted in the intact leg in addition to the paretic leg. Nevertheless, a relatively long recovery time, i.e., the period ranging from post-transfer to achieving skilled locomotion, was observed after the contralateral L4 transfer. Also, in the intact hindlimb, loss of motor function was observed after transecting L4, although it did not impair locomotion. Despite these shortcomings, neurotization still appears to be a promising approach (Saffari et al., 2020), and future studies should investigate if these effects on the intact limb could be overcome by advanced rehabilitation training and regeneration-promoting electrical stimulus (Hou et al., 2020; Wang et al., 2021).

Several limitations of this study need to be addressed in the future. In particular, no significant motion was observed in the digits post-intervention. It is possible that the short experiment duration did not allow enough time for this recovery. Additionally, the exact number of L4 nerve fibers on the intact side innervating the contralateral muscles and the ratios to other lumbar nerve roots were not quantified. Finally, as rats are quadrupeds, lower limbs are more frequently implicated in skilled motion in rats than in humans. Slight motor degradation tends to be more detectable in rats. However, the concept of the present study still applies to clinical practice.

In summary, contralateral L4 neurotization enabled motor recovery in the distal joint and improved performance in the proximal joints in a rat model of HICH. The findings suggest that this approach may be a therapeutic option for hindlimb paralysis secondary to HICH, which is supported by its feasibility and availability. Further research into the mechanisms underlying axonal regeneration and cortical plasticity in hindlimb recovery would be beneficial.

## References

Afshari FT, Hossain T, Miller C, Power DM (2019) Salvage of cervical motor radiculopathy using peripheral nerve transfer reconstruction. Br J Neurosurg 33:315-319.

Ahamed ZA, Sreejit MS (2019) Lumbar plexus block as an effective alternative to subarachnoid block for intertrochanteric hip fracture surgeries in the elderly. Anesth Essays Res 13:264-268.

Bao B, Fu K, Zheng X, Wei H, Luo P, Zhu H, Zhu X, Li X, Gao T (2020) Novel method for restoration of anorectal function following spinal cord injury via nerve transfer in rats. J Spinal Cord Med 43:177-184.

Chamudot R, Parush S, Rigbi A, Horovitz R, Gross-Tsur V (2018) Effectiveness of modified constraint-induced movement therapy compared with bimanual therapy home programs for infants with hemiplegia: a randomized controlled trial. Am J Occup Ther 72:7206205010p1-7206205010p9.

Chen CC, Chang CP (2020) Development of a three-channel automatic climbing training system for rat rehabilitation after ischemic stroke. Braz J Med Biol Res 53:e8943.

Chiaramonte R, Pavone P, Vecchio M (2020) Speech rehabilitation in dysarthria after stroke, a systematic review of the studies. Eur J Phys Rehabil Med 56:547-562.

Doi K, Sem SH, Hattori Y, Sakamoto S, Hayashi K, Maruyama A (2019) Contralateral obturator nerve to femoral nerve transfer for restoration of knee extension after acute flaccid myelitis: a case report. JBJS Case Connect 9:e0073.

Ettenhofer ML, Guise B, Brandler B, Bittner K, Gimbel SI, Cordero E, Nelson Schmitt S, Williams K, Cox D, Roy MJ, Chan L (2019) Neurocognitive Driving Rehabilitation in Virtual Environments (NeuroDRIVE): a pilot clinical trial for chronic traumatic brain injury. NeuroRehabilitation 44:531-544.

Fan W, Kuang X, Hu J, Chen X, Yi W, Lu L, Xu N, Wang L (2020) Acupuncture therapy for poststroke spastic hemiplegia: a systematic review and meta-analysis of randomized controlled trials. Complement Ther Clin Pract 40:101176.

Fernando SM, Tran A, Cheng W, Rochwerg B, Taljaard M, Kyeremanteng K, English SW, Sekhon MS, Griesdale DEG, Dowlatshahi D, McCredie VA, Wijdicks EFM, Almenawer SA, Inaba K, Rajajee V, Perry JJ (2019) Diagnosis of elevated intracranial pressure in critically ill adults: systematic review and meta-analysis. BMJ 366:l4225.

Fox I, Hoben G, Komaie G, Novak C, Hamm R, Kahn L, Whitehead M, Juknis N, Ruvinskaya R, Mackinnon S, James A (2019) Nerve transfer surgery in cervical spinal cord injury: a qualitative study exploring surgical and caregiver participant experiences. Disabil Rehabil 43:1542-1549.

Frost SB, Iliakova M, Dunham C, Barbay S, Arnold P, Nudo RJ (2013) Reliability in the location of hindlimb motor representations in Fischer-344 rats: laboratory investigation. J Neurosurg Spine 19:248-255.

Herweh C, Nordlohne S, Sykora M, Uhlmann L, Bendszus M, Steiner T (2017) Climatic and seasonal circumstances of hypertensive intracerebral hemorrhage in a worldwide cohort. Stroke 48:3384-3386.

Hirano Y, Nitta O (2020) Effects of nutritional status on prognosis in patients with severe hemiplegia who were recently admitted to a rehabilitation hospital. J Phys Ther Sci 32:319-322.

Hou X, Lv YF, Liu JM (2020) Meta-analysis of muscle strength of exercisers undergoing electrical muscle stimulation training. Zhongguo Zuzhi Gongcheng Yanjiu 24:3764-3772.

Jovanovic LI, Kapadia N, Lo L, Zivanovic V, Popovic MR, Marquez-Chin C (2020) Restoration of upper limb function after chronic severe hemiplegia: a case report on the feasibility of a brain-computer interface-triggered functional electrical stimulation therapy. Am J Phys Med Rehabil 99:e35-40.

Kemp SW, Alant J, Walsh SK, Webb AA, Midha R (2010) Behavioural and anatomical analysis of selective tibial nerve branch transfer to the deep peroneal nerve in the rat. Eur J Neurosci 31:1074-1090.

Kikuta S, Yalcin B, Iwanaga J, Watanabe K, Kusukawa J, Tubbs RS (2020) The supraorbital and supratrochlear nerves for ipsilateral corneal neurotization: anatomical study. Anat Cell Biol 53:2-7.

Lee SY, Amatya B, Judson R, Truesdale M, Reinhardt JD, Uddin T, Xiong XH, Khan F (2019) Applicability of traumatic brain injury rehabilitation interventions in natural disaster settings. Brain Inj 33:1293-1298.

Li P, Shen Y, Xu J, Liang C, Jiang S, Qiu Y, Yin H, Feng J, Li T, Shen J, Wang G, Yu B, Ye X, Yu A, Lei G, Cai Z, Xu W (2020) Contralateral cervical seventh nerve transfer for spastic arm paralysis via a modified prespinal route: a cadaveric study. Acta Neurochir (Wien) 162:141-146.

Lin H, Chen A, Hou C (2013) Contralateral L-6 nerve root transfer to repair lumbosacral plexus root avulsion: experimental study in rhesus monkeys. J Neurosurg 119:714-719.

Nath RK, Somasundaram C (2019) Functional improvement of upper and lower extremity after decompression and neurolysis and nerve transfer in a pediatric patient with acute flaccid myelitis. Am J Case Rep 20:668-673.

Niama Natta DD, Lejeune T, Detrembleur C, Yarou B, Sogbossi ES, Alagnidé E, Kpadonou T, Selves C, Stoquart G (2021) Effectiveness of a self-rehabilitation program to improve upper-extremity function after stroke in developing countries: a randomized controlled trial. Ann Phys Rehabil Med 64:101413.

Park C, Oh-Park M, Dohle C, Bialek A, Friel K, Edwards D, Krebs HI, You JSH (2020) Effects of innovative hip-knee-ankle interlimb coordinated robot training on ambulation, cardiopulmonary function, depression, and fall confidence in acute hemiplegia. NeuroRehabilitation 17:4291.

Paxinos G, Watson CR, Emson PC (1980) AChE-stained horizontal sections of the rat brain in stereotaxic coordinates. J Neurosci Methods 3:129-149.

Perin C, Bolis M, Limonta M, Meroni R, Ostasiewicz K, Cornaggia CM, Alouche SR, da Silva Matuti G, Cerri CG, Piscitelli D (2020) Differences in rehabilitation needs after stroke: a similarity analysis on the ICF core set for stroke. Int J Environ Res Public Health 17:4291.

Pino PA, Intravia J, Kozin SH, Zlotolow DA (2019) Early results of nerve transfers for restoring function in severe cases of acute flaccid myelitis. Ann Neurol 86:607-615.

Rivera-Lara L, Murthy SB, Nekoovaght-Tak S, Ali H, McBee N, Dlugash R, Ram M, Thompson R, Awad IA, Hanley DF, Ziai WC, Investigators C (2018) Influence of bleeding pattern on ischemic lesions after spontaneous hypertensive intracerebral hemorrhage with intraventricular hemorrhage. Neurocrit Care 29:180-188.

Saffari TM, Bedar M, Hundepool CA, Bishop AT, Shin AY (2020) The role of vascularization in nerve regeneration of nerve graft. Neural Regen Res 15:1573-1579.

Sananpanich K, Kraisarin J, Siriwittayakorn W, Tongprasert S, Suwansirikul S (2018) Double motor nerve transfer for all finger flexion in cervical spinal cord injury: an anatomical study and a clinical report. J Hand Surg 43:920-926.

Schiavo S, Richardson D, Santa Mina D, Buryk-Iggers S, Uehling J, Carroll J, Clarke H, Djaiani C, Gershinsky M, Katznelson R (2020) Hyperbaric oxygen and focused rehabilitation program: a feasibility study in improving upper limb motor function after stroke. Appl Physiol Nutr Metab 45:1345-1352.

Simpson DB, Breslin M, Cumming T, de Zoete SA, Gall SL, Schmidt M, English C, Callisaya ML (2021) Sedentary time and activity behaviors after stroke rehabilitation: changes in the first 3 months home. Top Stroke Rehabil 28:42-51.

Song H, Jung W, Lee E, Park JY, Kim MS, Lee MC, Kim HI (2017) Capsular stroke modeling based on somatotopic mapping of motor fibers. J Cereb Blood Flow Metab 37:2928-2937.

Song RB, Basso DM, da Costa RC, Fisher LC, Mo X, Moore SA (2016) Adaptation of the Basso-Beattie-Bresnahan locomotor rating scale for use in a clinical model of spinal cord injury in dogs. J Neurosci Methods 268:117-124.

Tiwari E, Salvadeo DM, Braverman AS, Frara NA, Hobson L, Cruz G, Brown JM, Mazzei M, Pontari MA, White AR, Barbe MF, Ruggieri MR (2019) Nerve transfer for restoration of lower motor neuron-lesioned bladder and urethra function: establishment of a canine model and interim pilot study results. J Neurosurg Spine 32:258-268.

Tuffaha SH, Meaike JD, Moran SL (2020) Direct muscle neurotization with long acellular nerve allograft: a case report. Microsurgery 40:258-260.

Wang CY, Miyoshi S, Chen CH, Lee KC, Chang LC, Chung JH, Shi HY (2020) Walking ability and functional status after post-acute care for stroke rehabilitation in different age groups: a prospective study based on propensity score matching. Aging (Albany NY) 12:10704-10714.

Wang S, Zhang LC, Fu HT, Deng JH, Xu GX, Li T, Ji XR, Tang PF (2021) Epidural electrical stimulation effectively restores locomotion function in rats with complete spinal cord injury. Neural Regen Res 16:573-579.

Werner JM, Berggren J, Kim G, Loffredo K, Pascual M, Tiongson E, Seruya M (2021) Recommendations for therapy following nerve transfer for children with acute flaccid myelitis. Phys Occup Ther Pediatr 41:209-226.

Yang F, Chen L, Wang H, Zhang J, Shen Y, Qiu Y, Qu Z, Li J, Xu W (2021) Combined contralateral C7 to C7 and L5 to S1 cross nerve transfer for treating limb hemiplegia after stroke. Br J Neurosurg doi: 10.1080/02688697.2021.1910764.

Yang K, Jiang F, Zhang S, Zhao H, Shi Z, Liu J, Cao X (2020) Extradural contralateral C7 nerve root transfer in a cervical posterior approach for treating spastic limb paralysis: a cadaver feasibility study. Spine (Phila Pa 1976) 45:E608-615.

Yorukoglu UH, Gurkan Y (2018) Combined quadratus lumborum block and lumbar plexus block for a pediatric patient undergoing Ilizarov procedure. J Clin Anesth 49:40-41.

Yu AP, Jiang S, Zhao HL, Liang ZH, Qiu YQ, Shen YD, Wang GB, Liang C, Xu WD (2019a) Application of CUBE-STIR MRI and high-frequency ultrasound in contralateral cervical 7 nerve transfer surgery. Br J Neurosurg doi: 10.1080/02688697.2019.1584661.

Yu BF, Chen LW, Qiu YQ, Xu J, Yin HW, Li QY, Xu WD (2019b) Contralateral seventh cervical nerve transfer can affect the pennation angle of the lower limb in spastic hemiplegia patients: An observational case series study. Brain Behav 9:e01460.

Yu BF, Qiu YQ, Du MX, Yin HW, Shen J, Ye X, Cai ZY, Xu WD (2020) Contralateral hemi-fifth-lumbar nerve transfer for unilateral lower limb dysfunction due to incomplete traumatic spinal cord injury: a report of two cases. Microsurgery 40:234-240.

Zheng MX, Hua XY, Feng JT, Li T, Lu YC, Shen YD, Cao XH, Zhao NQ, Lyu JY, Xu JG, Gu YD, Xu WD (2018a) Trial of contralateral seventh cervical nerve transfer for spastic arm paralysis. New Engl J Med 378:22-34.

Zheng MX, Hua XY, Jiang S, Qiu YQ, Shen YD, Xu WD (2018b) Contralateral peripheral neurotization for a hemiplegic hindlimb after central neurological injury. J Neurosurg 128:304-311.

Zhu Z, Bower M, Stern-Nezer S, Atallah S, Stradling D, Groysman L, Dastur CK, Akbari Y, Yu W (2020) Early initiation of oral antihypertensives reduces intensive care unit stay and hospital cost for patients with hypertensive intracerebral hemorrhage. Neurocrit Care 32:707-714.

Zong H, Ma F, Zhang L, Lu H, Gong J, Cai M, Lin H, Zhu Y, Hou C (2016) Hindlimb spasticity after unilateral motor cortex lesion in rats is reduced by contralateral nerve root transfer. Biosci Rep 36:e00430.